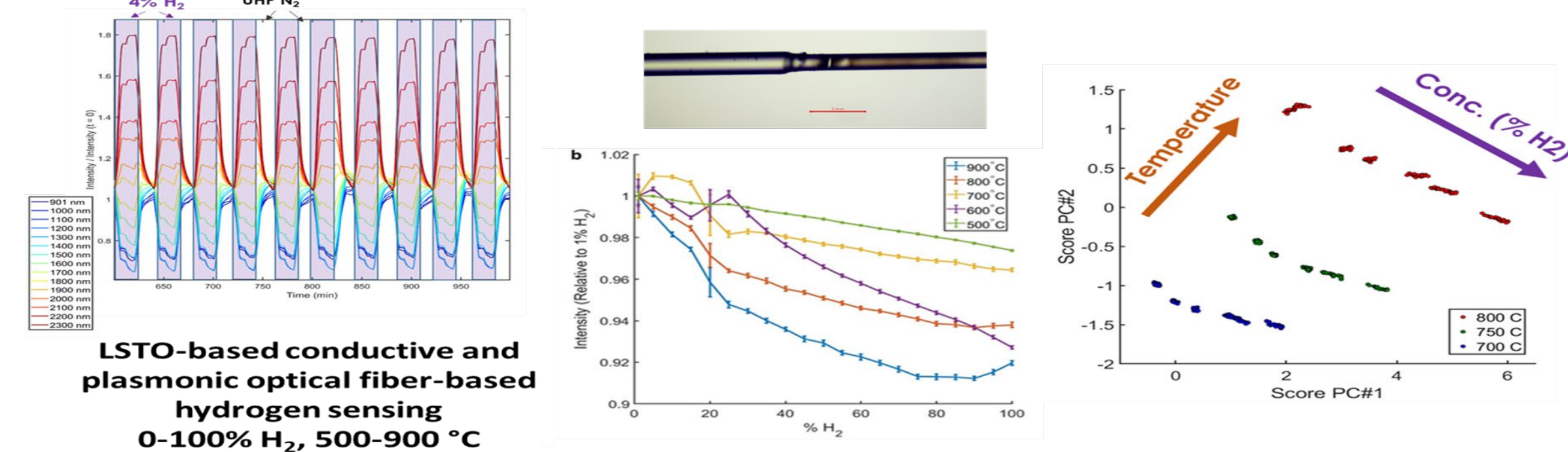


Introduction

- For advanced real-time monitoring and control of gas species in combustion environments, development of efficient sensing platforms and new sensor materials able to work under harsh environments are required.
- Semiconducting optical-based sensor platforms show promise. MO_x metal-oxides and ABO₃ perovskite-oxides can be attractive for high-temperature applications due to their high decomposition temperatures and structural stability; La-doped SrTiO₃ acts like an n-type doped semiconductor under reducing conditions – demonstrating an effective high-T sensing material for H₂.



ML in Perovskite Oxide Design



1 Material Generation

- ~190 million ABO₃ compositions: 13 A-site × 36 B-site elements
- 1-2 element with 0.7-1.0 total A/B site ratio

2 Perovskite Stability Prediction

- Gradient Boosting Classifier reduced candidates to ~40 million
- Trained on ~1,000 verified ABO₃
- Classifier features: bond distances, Mendeleev numbers, oxidation states, and variance factors

3 Conductivity Prediction

- XGBoost Regressor predicts conductivity of ABO₃ compositions, at oxygen partial pressures (pO₂) and temperatures
- Trained on over 7,000 experimental conductivity data
- Features: Magnetic moment, ionic radius, electronegativity, cell volume, band gap, formation energy, and atomic mass

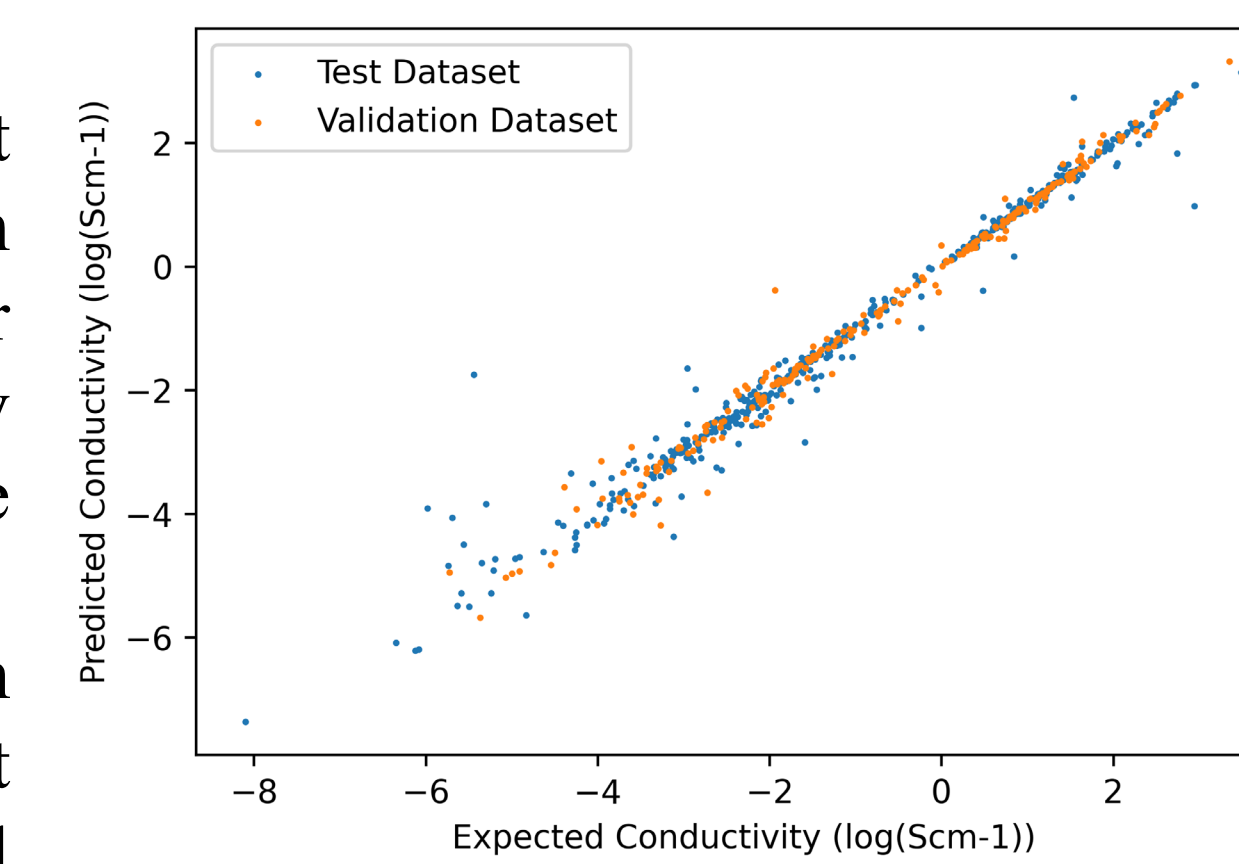
4 Conductivity Sensitivity Ranking

- Identifying materials with significant conductivity changes due to oxygen partial pressure at specific temperatures ($\partial \log(\sigma) / \partial \log(pO_2)$ metric)

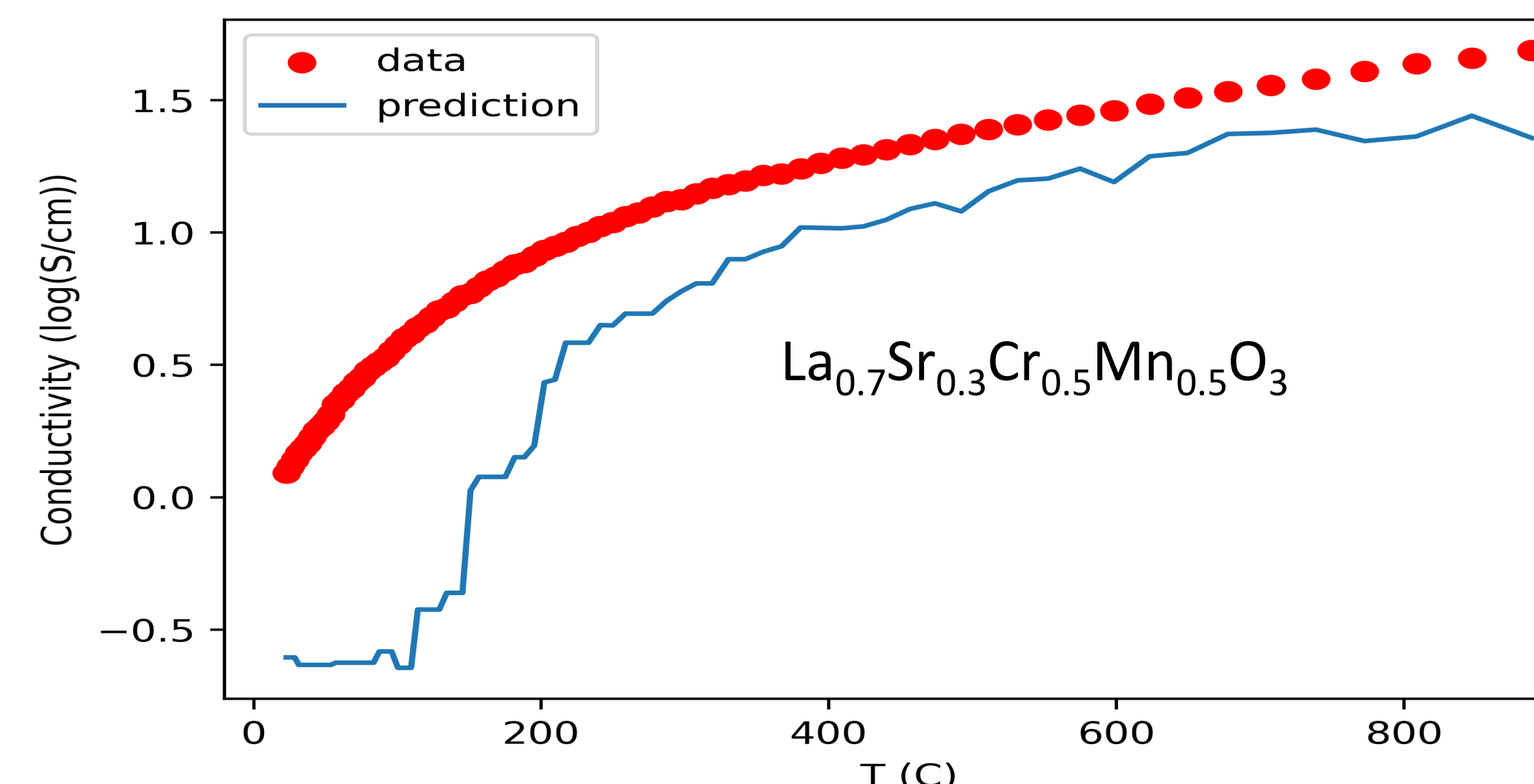
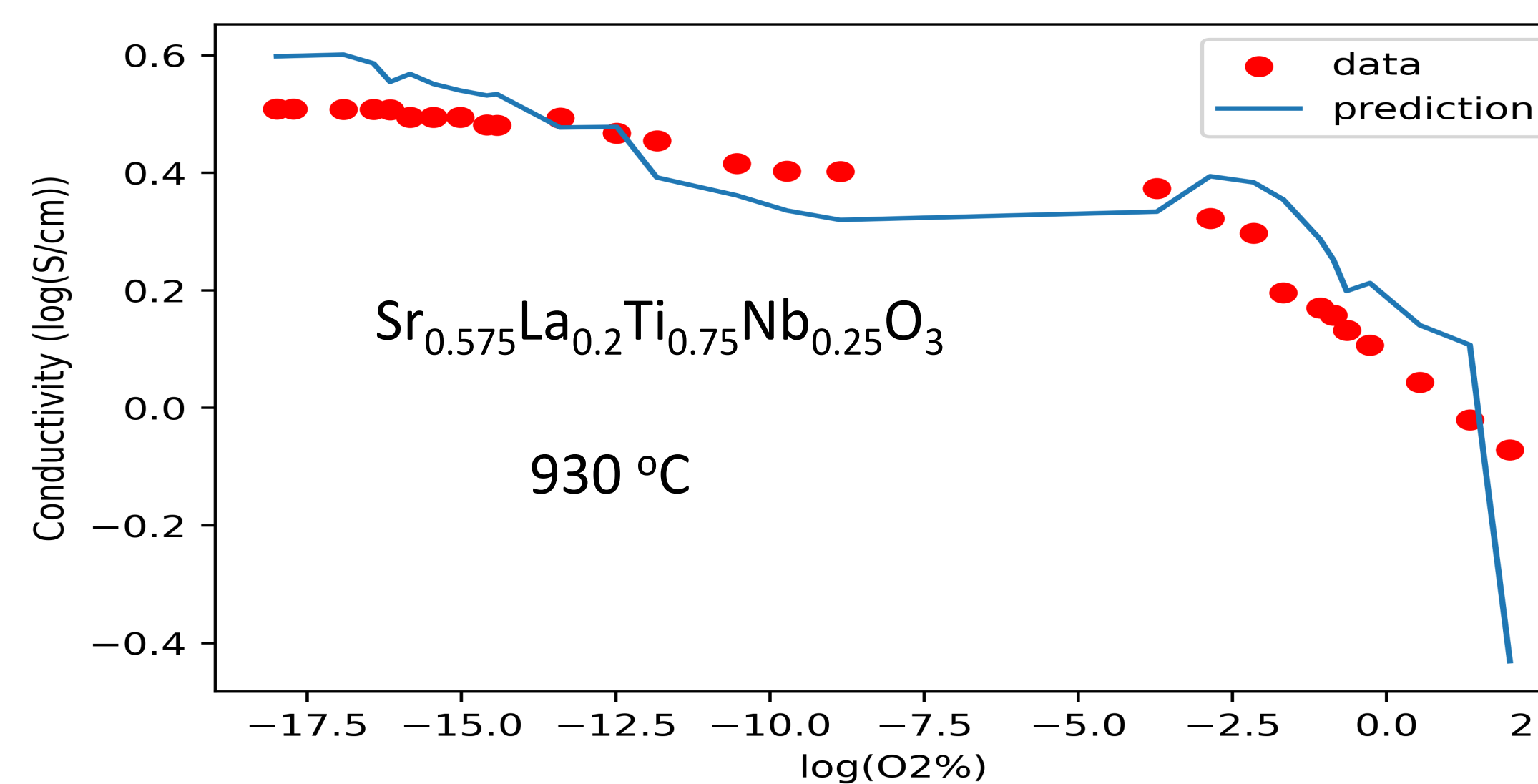
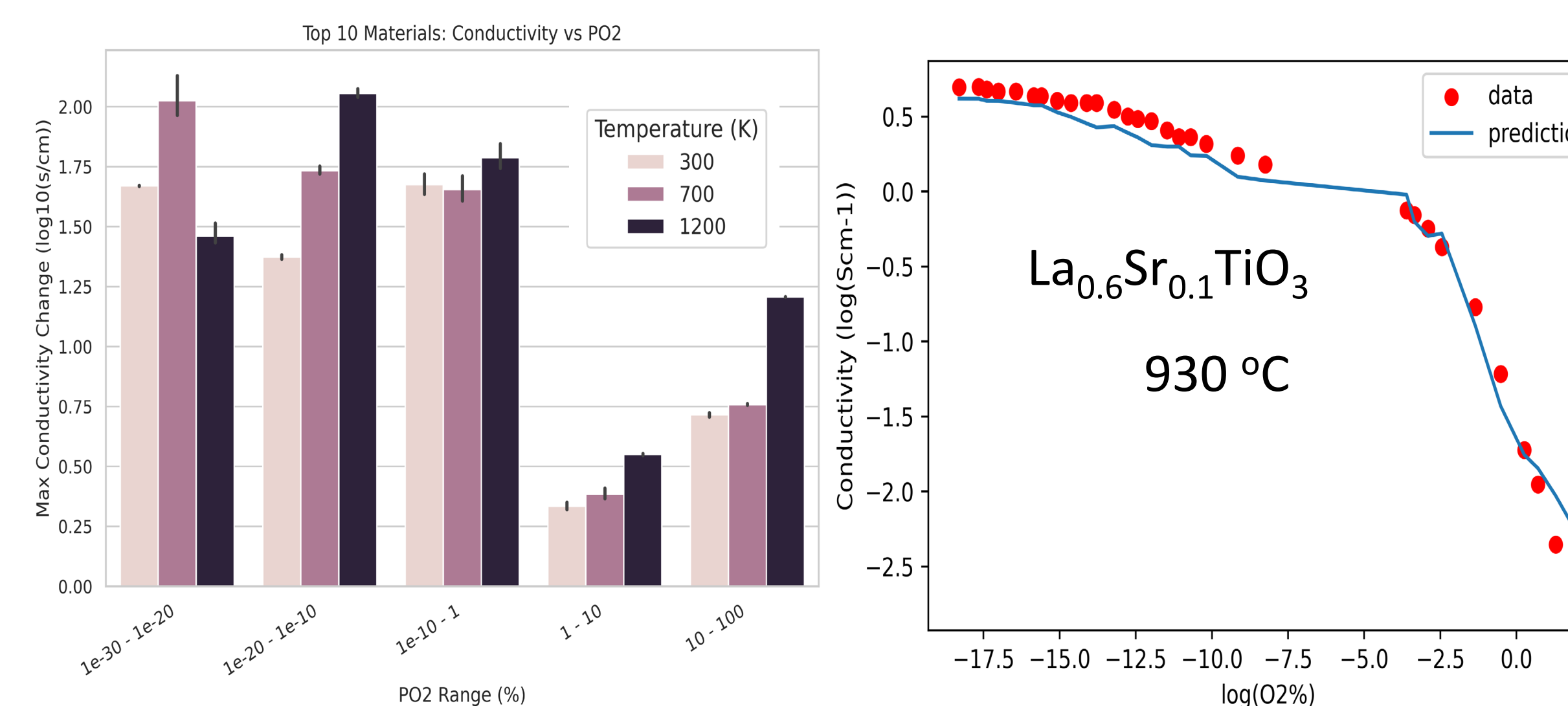
Conductivity Prediction

ML with perovskite database

- Priya et al trained XG boost regressor model with perovskite database of over 7,230 experiment conductivity data points across 415 unique compositions
- 110 features derived from Materials Project & element data as well as O₂ partial pressure & temperature

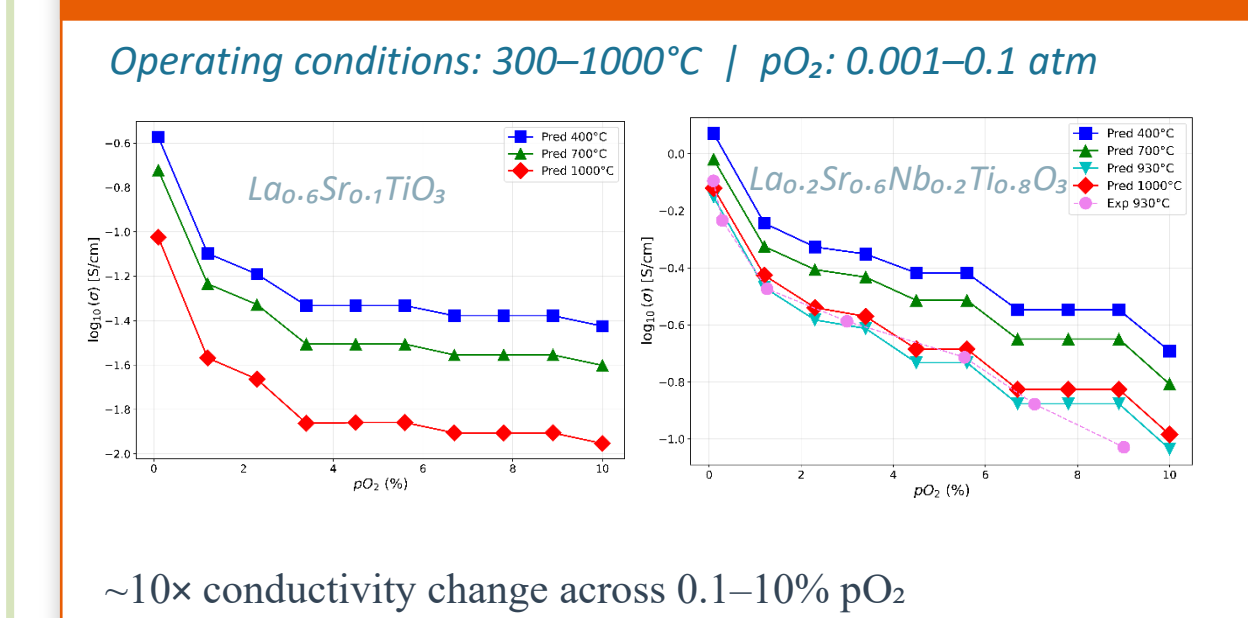


Priya, P. and Aluru, N.R., *npj Computational Materials*, 7(2021)90.
Zhai, Ximei, et al. *Communications Materials* 3(2022)42.



Industrial Applications

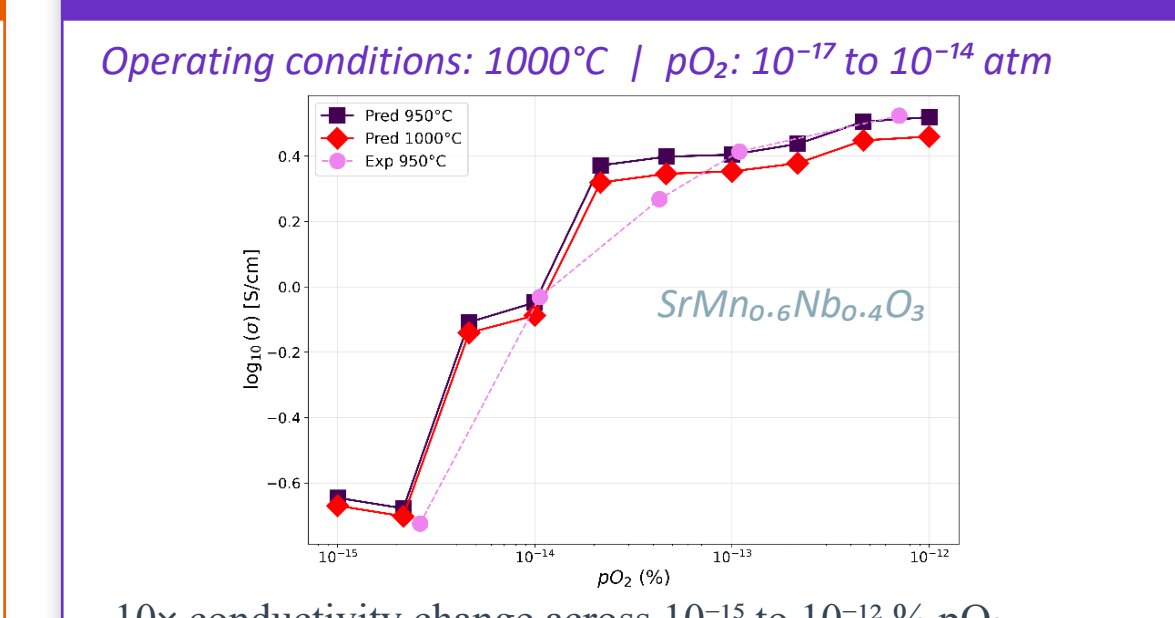
AUTOMOTIVE EXHAUST GAS MONITORING



~10x conductivity change across 0.1-10% pO₂

| Top 5 @ 700°C | Δ log(σ) |
|--|----------|
| La _{0.6} Sr _{0.1} TiO ₃ | 0.88 |
| La _{0.2} Sr _{0.6} Nb _{0.2} Ti _{0.8} O ₃ | 0.79 |
| La _{0.55} Sr _{0.15} Nb _{0.05} Ti _{0.95} O ₃ | 0.71 |
| La _{0.5} Sr _{0.15} TiO ₃ | 0.70 |
| La _{0.4} Sr _{0.4} TiO ₃ | 0.69 |

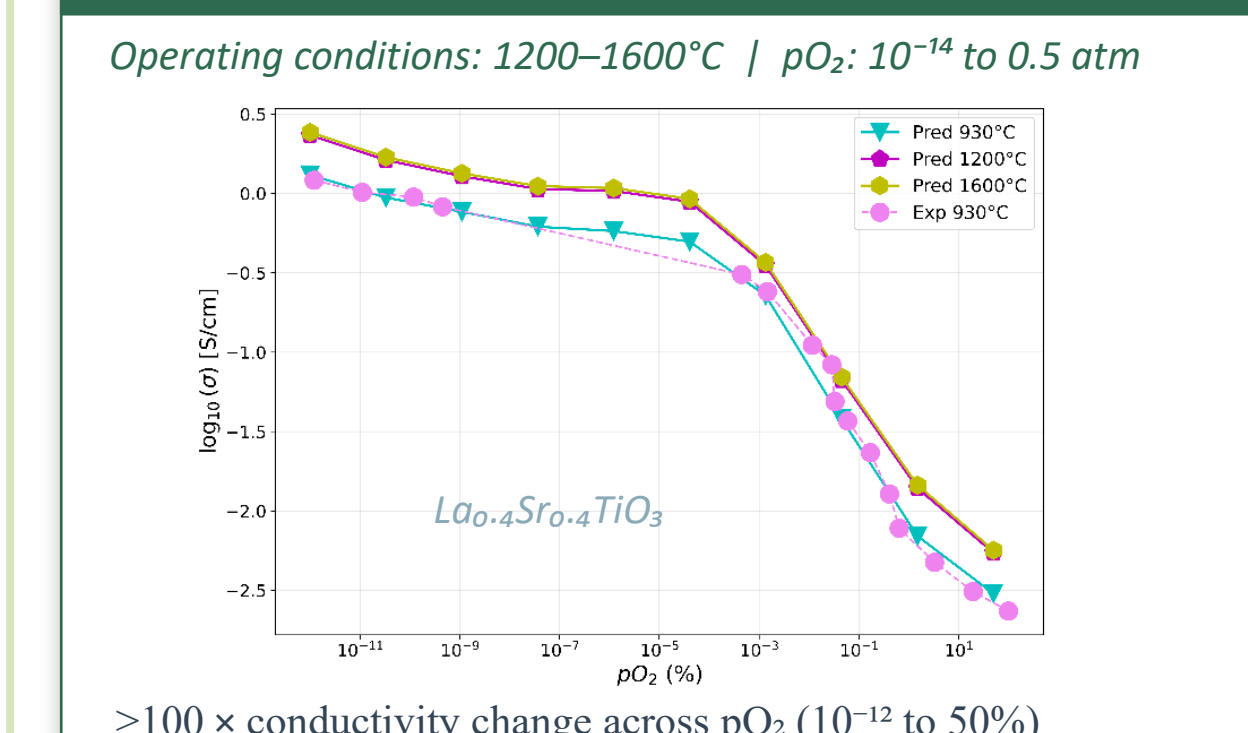
STEEL MANUFACTURING FURNACES



~10x conductivity change across 10⁻¹⁵ to 10⁻¹² % pO₂

| Top 5 @ 1000°C | Δ log(σ) |
|--|----------|
| SrMn _{0.6} Nb _{0.4} O ₃ | 1.13 |
| Ca _{0.05} Sr _{0.95} Mn _{0.6} Nb _{0.4} O ₃ | 1.06 |
| Sr _{0.8} Yb _{0.2} Mn _{0.65} Nb _{0.05} O ₃ | 1.05 |
| Sr _{0.7} Yb _{0.3} Mn _{0.65} Nb _{0.05} O ₃ | 1.05 |
| Sr _{0.55} Yb _{0.15} Mn _{0.65} Nb _{0.05} O ₃ | 1.04 |

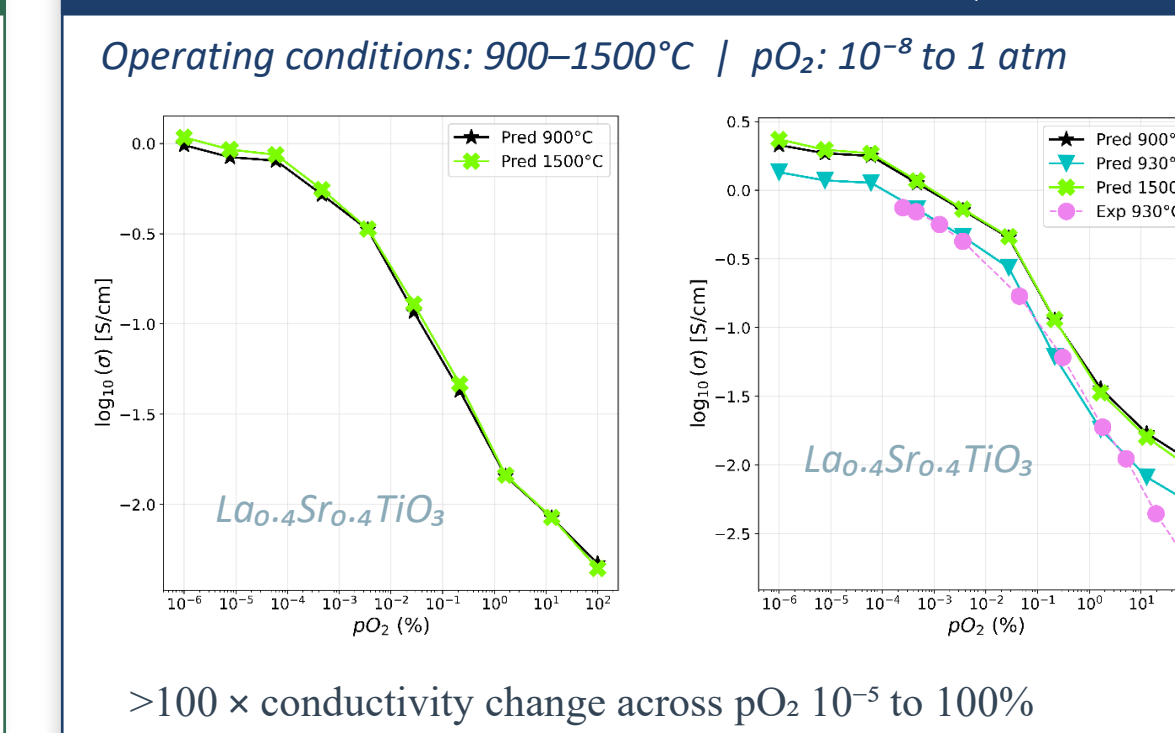
GLASS MANUFACTURING



>100 x conductivity change across pO₂ (10⁻¹² to 50%)

| Top 5 @ 1200°C | Δ log(σ) |
|---|----------|
| La _{0.4} Sr _{0.4} TiO ₃ | 2.52 |
| La _{0.6} Sr _{0.1} TiO ₃ | 2.52 |
| La _{0.45} Sr _{0.55} TiO ₃ | 2.41 |
| La _{0.55} Sr _{0.15} TiO ₃ | 2.39 |
| Ba _{0.25} Y _{0.45} Nb _{0.05} Ti _{0.95} O ₃ | 2.37 |

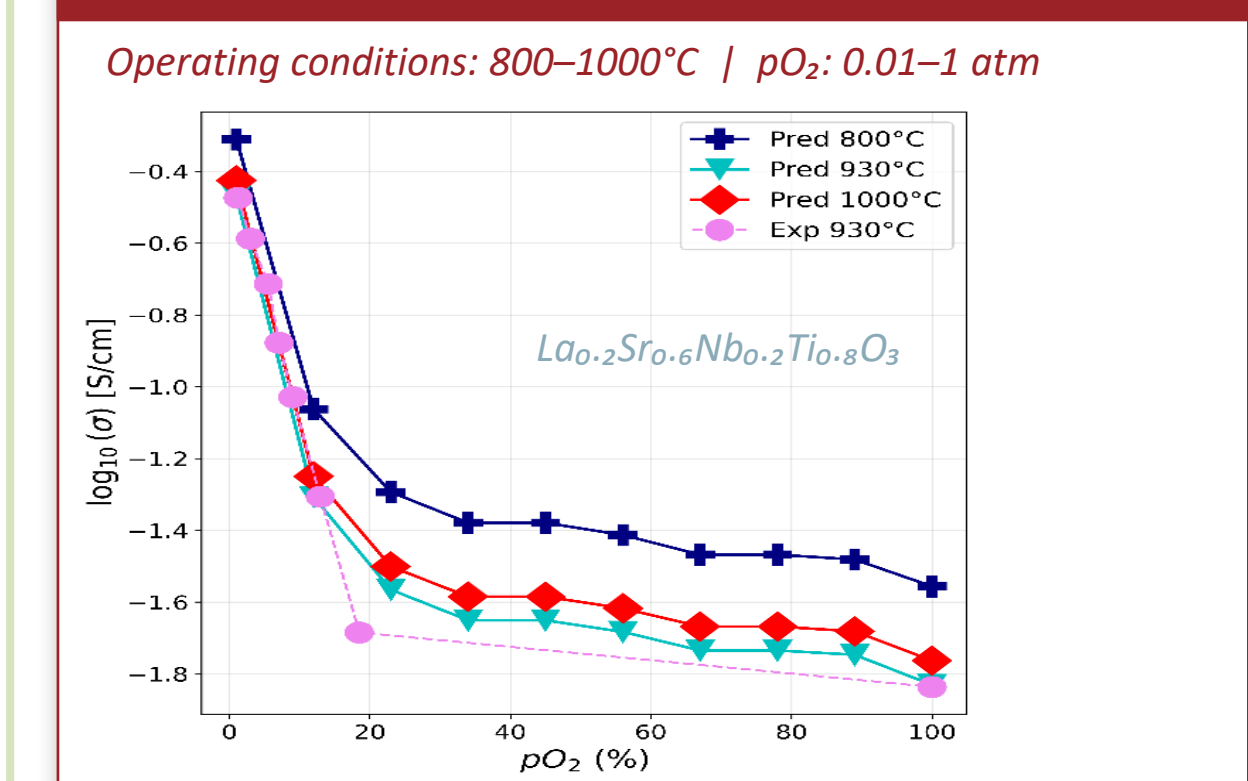
SEMICONDUCTOR PROCESSING (SiC MOS)



>100 x conductivity change across pO₂ 10⁻⁵ to 100%

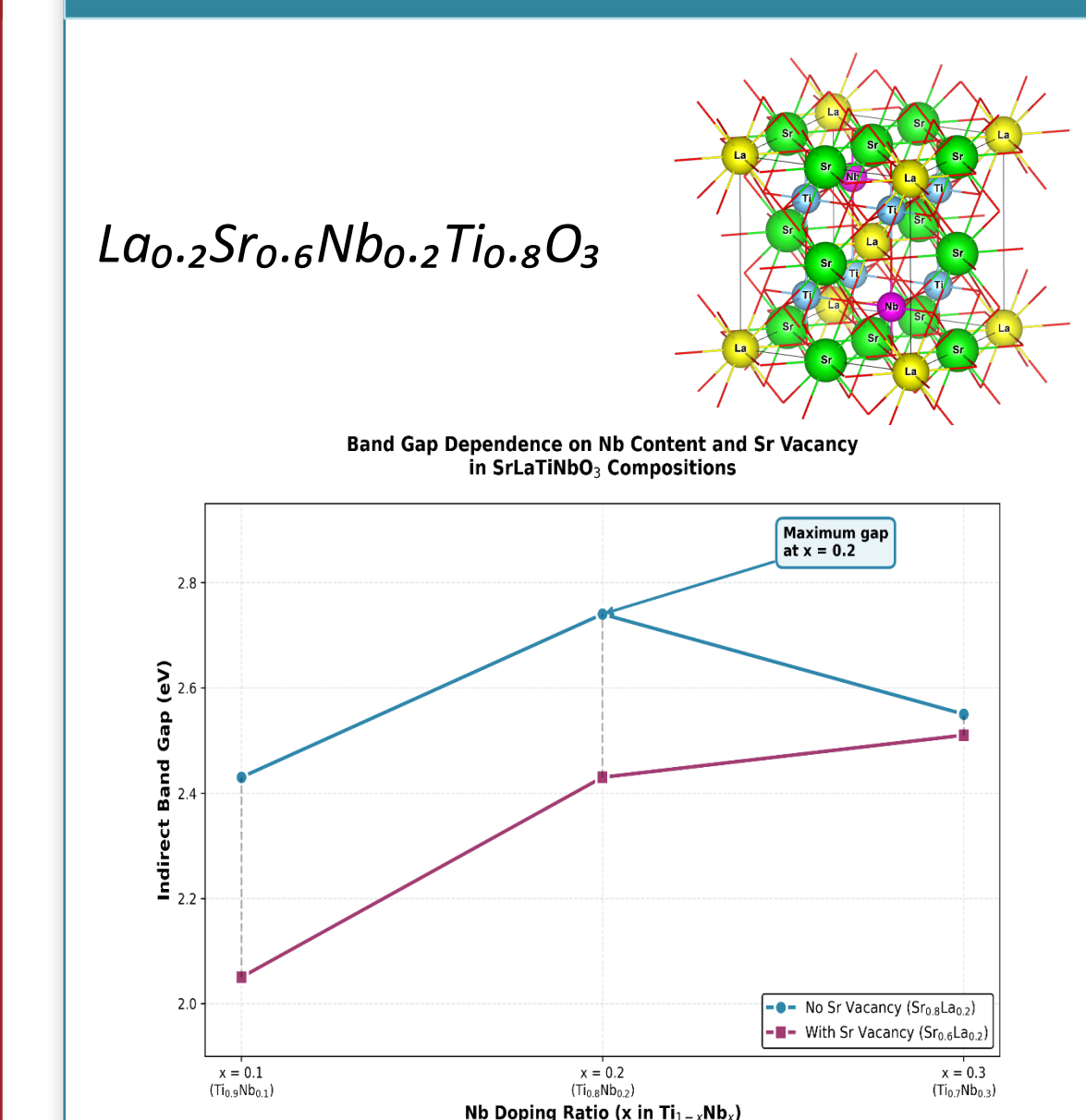
| Top 5 @ 900°C | Δ log(σ) |
|--|----------|
| La _{0.4} Sr _{0.4} TiO ₃ | 2.32 |
| La _{0.6} Sr _{0.1} TiO ₃ | 2.31 |
| La _{0.55} Sr _{0.15} TiO ₃ | 2.18 |
| La _{0.25} Sr _{0.55} Nb _{0.15} Ti _{0.85} O ₃ | 2.15 |
| La _{0.3} Sr _{0.3} Nb _{0.15} Ti _{0.85} O ₃ | 2.14 |

Pt THIN-FILM RESISTOR PROCESSING



| Top 5 @ 1000°C | Δ log(σ) |
|--|----------|
| La _{0.2} Sr _{0.6} Nb _{0.2} Ti _{0.8} O ₃ | 1.34 |
| Nd _{0.85} Pr _{0.15} AlO ₃ | 1.25 |
| Nd _{0.9} Pr _{0.1} AlO ₃ | 1.25 |
| Gd _{0.15} La _{0.85} AlO ₃ | 1.25 |

DFT MODELLING



Publications

- J. Park *et al.*, *Phys. Chem. Chem. Phys.* 22(2020) 27163-72; *ACS Appl. Mater. Interfaces* 13(2021) 17717-25; *J. Phys. Chem. C* 125(2021) 22231-38; 126(2022)8832-38; *Chem. Mater.* 34(2022)6108-15
- Y.-N. Wu *et al.*, *J. Phys. Chem. C* 122(2018) 22642-49; *J. Phys. Chem. Lett.* 11(2020) 2518-23; *J. Phys. Condens. Matter* 32(2020) 405705.
- T. Jia *et al.*, *RSC Adv.* 7(2017) 38798-804; *Phys. Chem. Chem. Phys.* 22(2020) 16721-26; *Applied Energy* 281(2021)116040; *J. Phys. Chem. C* 125(2021) 12374-81; 126(2022)11421-25
- Y. Duan *et al.*, *J. Solid State Chem.* 256(2017) 239-251.
- S. Nations, *et al.*, *RSC Adv.* 11(2021) 22264-72; *Mater. Adv.* 3(2022)3897-3905; *Nanomaterials* 13(2023)276
- T. Nandi, L. Chong, J. Park, W. A. Saidi, B. Chorpeneing, S. Bayham, Y. Duan, *AIP Advances* 14(3)(2024)035231